Effect of Strain on Grain and Grain-Boundary Critical Currents of YBCO Coated Conductors

A. Palau, T. Puig, X. Obradors, R. Feenstra, and H. C. Freyhardt

***Abstract*—We present a comparative analysis on tensile strain tolerance of critical currents for IBAD and RABiTS coated conductors. These measurements have been performed with a recently developed methodology based on dc-magnetization measurements, which enables us to analyze the grain and grain-boundary critical current densities simultaneously. We show that the percolative grain-boundary critical current density may be reduced by 50% with deformations of $\varepsilon \sim 0.32\%$ and 1% for RABiTS and IBAD, respectively, while the grain critical current and thus the pinning properties of the grains are not affected by the deformation process.**

***Index Terms*—Coated conductor, critical current, deformation process, strain tolerance.**

I. Introduction

COATED conductors have emerged as a promising material for long length biaxially textured HTSC wires operating in high magnetic fields, such as windings for motors, generators, and magnets. In all of these applications, the conductor is submitted to large stresses so that it has to be flexible and able to support mechanical deformations without major deterioration of the transport properties. Due to its granular microstructure and the strong dependence of critical current density J_c on grain misorientations, the transport current in coated conductors (CC) flows in a percolative way through the network of grain boundaries [1]–[3]. Therefore, J_c can be limited by two different mechanisms: vortex pinning associated with the grain critical current density, $J_c{}^{G}$, and percolative issues associated with the grain boundary network, $J_c{}^{GB}$. The ability to transport large current densities ($J_c{}^{GB} \sim 2-3\ MA/cm^2$ at 77 K) is sustained by ensuring excellent grain-to-grain alignment and of course a good connection between grains, without crack formation at the grain boundaries. To deal with this issue and characterize the maximum stresses that can be applied to YBCO coated conductors, we have studied the evolution of $J_c{}^{GB}$ and $J_c{}^{G}$ after mechanical deformation of the tapes. Coated conductors with different substrate architectures, RABiTS and IBAD CCs, have been considered in order to evaluate the strain tolerance in each case. Previous studies of strain effects in YBCO coated conductors have shown a degradation of the transport critical current density upon a deformation process caused by the formation of cracks [4]–[7]. In this paper we are able to conclude on a correlation between $J_c{}^{G}$ and $J_c{}^{GB}$ with the induced deformation, derived from simultaneous measurements.

Manuscript received October 5, 2001. This work was supported by MCyT (MAT2002-02642), Generalitat de Catalunya (SRG2001-00189 and CeRMAE) and EU (SOLSULET G5RD-CT2001-00550).

A. Palau, T. Puig, and X. Obradors are with the Institut de Ciència de Materials de Barcelona, CSIC, Campus UAB, 08193 Bellaterra, Spain (e-mail: palau@icmab.es).

R. Feenstra is with Oak Ridge National Laboratory, Oak Ridge, TN 37831-6057 USA.

H. C. Freyhardt is with the Zentrum fur FunktionWekstoffe, 37073 Göttingen, Germany.

Digital Object Identifier 10.1109/TASC.2005.848214

II. Experimental Details

High-quality IBAD and RABiTS coated conductors have been analyzed. Results are presented for a YBCO-RABiTS sample which is a 0.63 μm thick YBCO film grown by a BaF_2 ex situ process using evaporated precursors on a CeO_2 (0.015 μm)/ YSZ (0.15 μm)/ Y_2O_3 (0.02 μm) / Ni (1.5μm)/Ni − 3%W-RABiTS tape (50 μm) [8] and a second YBCO-IBAD sample prepared by depositing 1 μm thick YBCO film by high rate pulsed laser deposition (PLD) on CeO_2 (0.9 μm)/IBAD-YSZ (1 μm)/Ni-Cr stainless steel substrate (100 μm) [9]. Bending tests have been performed on both samples. The tests consisted of winding the samples around cylinders of different radius, ρ, with the YBCO layer facing outside and inducing a tensile bend strain. Thus, the applied strain was increased by decreasing the cylinder radius. The bend strain tolerance has been characterized as a percent deformation, ε, calculated, assuming a tape with homogeneous mechanical properties, $\varepsilon = t/2\rho$, where t is the tape thickness, that is much smaller than the bending diameter [5]. However, the actual strain experienced by the YBCO layer could be less than ε because of the different mechanical properties of the metallic substrate and the oxide layers. Grain and grain-boundary critical current densities, $J_c{}^{G}$ and $J_c{}^{GB}$, of YBCO RABiTS and IBAD CCs as grown and after bending tests have been determined simultaneously by applying the inductive methodology recently reported [10]. Zero field cooled magnetic hysteresis loops were measured with a Quantum Design SQUID provided with a 7 T superconducting coil on samples of 5 mm × 5 mm. Subtraction of the substrate magnetic signal was carried out for all cases.

III. Results and Discussion

In Fig. 1 we present the reverse branch of several hysteresis loops measured for the RABiTS and IBAD conductors before the bending tests, at 77 K. As it was reported in A. Palau *et al.* [10], the maximum of the saturated reverse branch of the magnetization curve of any CC is not observed at a zero applied field, $\mu_0 H_a = 0$, as one should expect for an epitaxial thin film, but at a positive applied magnetic field. This effect was shown to be a clear confirmation of the magnetic granular structure of CCs and it was attributed to the fact that the magnetic

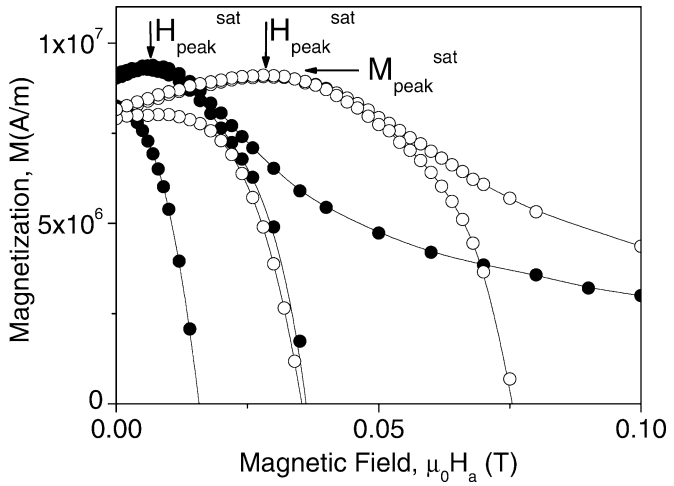

Fig. 1. Reverse branches of several magnetic hysteresis loops measured at 77 K for IBAD-CC with $\mu_0 H_m$ =0.02 T, 0.04 T and 0.2 T (■) and RABiTS-CC with $\mu_0 H_m$ =0.04 T, 0.08 T and 0.2 T (∘).

field trapped into the grains was returning through the GBs, $\mu_0 H_{return}$, thus generating a reduced local magnetic field at the GBs, $\mu_0 {H_{loc}}^{GB} = \mu_0(H_a - H_{return})$. When $\mu_0 {H_{loc}}^{GB} \sim 0$ the magnetization peaks and $\mu_0 H_{peak} \sim \mu_0 H_{return}$. The value of $\mu_0 H_{peak}$ increases as one increases the maximum applied field in the hysteresis loop, $\mu_0 H_m$, and then it saturates, when the grain magnetization at this position saturates. The maximum magnetic field needed to saturate the grain magnetization, at zero applied field, $\mu_0 {H_m}^{sat}$, is a measurement of the grain full penetration field $\mu_0 H_G{}^*$, i.e. $\mu_0 {H_m}^{sat} \sim \mu_0 2H_G{}^*$ [10], [11]. The two experimental magnetic field values, $\mu_0 {H_{peak}}^{sat}$ and $\mu_0 {H_m}^{sat}$, can be used to determine the grain critical current density, ${J_c}^G$, and the average magnetic grain size, $\langle 2a \rangle$, of each CC [10]. Notice that whereas both samples exhibit a peak of the magnetization, at $\mu_0 H_a > 0$, the value of $\mu_0 {H_{peak}}^{sat}$ is different in each case. For the IBAD-CC $\mu_0 {H_{peak}}^{sat}$ appears at 0.007 T while for RABiTS-CC $\mu_0 {H_{peak}}^{sat} \sim 0.028$ T. Additionally, the maximum magnetic field that had to be applied in order to saturate the grain magnetization at zero applied field was $\mu_0 {H_m}^{sat} \sim 0.04$ T and 0.052 T, for the IBAD and RABiTS-CCs, respectively. With these values one can calculate the ratio ${H_{peak}}^{sat}/{H_m}^{sat}$, to estimate the superconducting average grain size for each type of CC using (1) [10],

$$\frac{{H_{peak}}^{sat}}{{H_m}^{sat}} = g\,(a/L) \tag{1}$$

where a is the grain radius, L the YBCO superconducting film thickness and g(a/L) is a numerical dimensionless calculated factor which increases with the ratio a/L. The smaller ratio for the IBAD sample, ${H_{peak}}^{sat}/{H_m}^{sat} \sim 0.2$, results in a smaller grain size of about, $\langle 2a \rangle \sim 2\,\mu m$, whereas for the RABiTS CC, with ${H_{peak}}^{sat}/{H_m}^{sat} \sim 0.54$, one obtains, $\langle 2a \rangle \sim 25\,\mu m$, in agreement with the structural grain size determined by TEM and EBSD (Electron Backscattering Diffraction) [12], [13]. With the average grain size and the experimental value $\mu_0 {H_{peak}}^{sat}$, the grain critical current density is determined, ${J_c}^G$, by means of (2) [10],

$${J_c}^G = \frac{{H_{peak}}^{sat}}{xL} \tag{2}$$

where x is a numerically calculated dimensionless factor which depends on the ratio a/L. The values of ${J_c}^G$ obtained for RABiTS and IBAD CCs before the bending tests are very similar, at 77 K, ${J_c}^G = 3.4\ MA/cm^2$ and $3.0\ MA/cm^2$, respectively. These results indicate that the superconductor grains exhibit similar flux pinning capabilities although they have been grown with different techniques. Additionally the percolative critical current density, associated to the GB network, ${J_c}^{GB}$, can be determined using magnetization measurements shown in Fig. 1 and the standard critical state equation for a disc [10],

$${J_c}^{GB} = \frac{3{M_{peak}}^{sat}}{R_s} \tag{3}$$

where ${M_{peak}}^{sat}$ is the saturated value of the magnetic moment at the peak, i.e. when $\mu_0 {H_{loc}}^{GB} \sim 0$, and R_s is the total sample radius. Before performing the bending tests, very similar values of ${J_c}^{GB}$ have also been obtained, ${J_c}^{GB} = 1.7\ MA/cm^2$ and $1.3\ MA/cm^2$ for the RABiTS and IBAD CCs, respectively. Notice that the ${J_c}^{GB}$ values are just two or three times smaller than the corresponding ${J_c}^G$ values, indicating that these coated conductors are of very high quality. Starting from RABiTS and IBAD CCs of very similar quality, bending test with cylinders of different radius have been performed for both samples in order to study the evolution of ${J_c}^{GB}$ and ${J_c}^G$ with the bending strain. The inset of Fig. 2 shows the reverse branch of the saturated magnetization hysteresis loops measured for the RABiTS CC at 77 K, as grown, $\varepsilon = 0\%$, and after three consecutive bendings around cylinders of radius, $\rho = 0.8$ cm, 0.62 cm and 0.4 cm, which corresponds to induced deformations of $\varepsilon = 0.32\%$, 0.4% and 0.62%. Notice that an important reduction of the magnetization is observed after each bending which is associated to a decrease in ${J_c}^{GB}$ according to (3). However, when the reverse curves are normalized to the corresponding magnetization value at the peak position (Fig. 2), one can observe that the magnetization peak appears at exactly the same applied magnetic field, $\mu_0 {H_{peak}}^{sat}$, for all the hysteresis loops. It was also confirmed that the saturation of the grain magnetization takes place at the same maximum applied field, $\mu_0 {H_m}^{sat}$. Therefore, one can conclude from (1) and (2) that the grain size, $\langle 2a \rangle$, and the grain critical current density, ${J_c}^G$, stay constant during all the bending process. The same strain deformation process has been performed to the IBAD-CC. The inset of Fig. 3 shows the resultant reverse branches of the magnetization loops at 77 K obtained before the bending tests, $\varepsilon = 0\%$, and after the induced deformations of $\varepsilon = 0.63\%$, 0.8%, 1.25% and 2.6%. Comparing these curves with the ones measured for the RABiTS tape (Inset of Fig. 2) we observe that for the IBAD sample, the magnetization also decreases after each bending process but the strain needed to obtain the same reduction in magnetization is higher. This corresponds to a faster degradation of ${J_c}^{GB}$ with the bending strain for the RABiTS tape than for the IBAD, as it is shown in Fig. 5. From the normalized reverse magnetization curves obtained for the IBAD-CC shown in Fig. 3 one observes that the magnetization does not peak at the same applied field after the bending tests, as observed for the RABiTS-CC, but rather the peak moves to higher magnetic fields when the sample is bent, $\mu_0 {H_{peak}}^{sat} = 0.007$ T, 0.008 T, 0.01 T, 0.013 T and 0.013 T for $\varepsilon = 0\%$, 0.63%, 0.8%, 1.25%

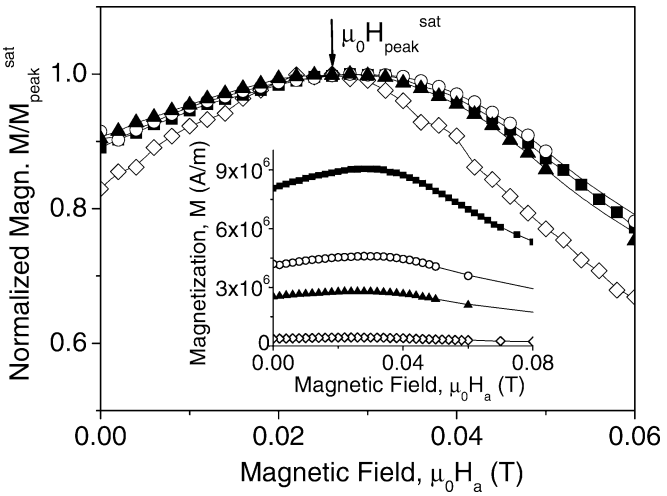

Fig. 2. Saturated reverse branches of the magnetization curves normalized to the corresponding magnetization value at the peak position, obtained for the RABiTS-CC at 77 K, as grown (■) and after consecutive bending with induced deformations of $\varepsilon = 0.32\%$ (∘), $\varepsilon = 0.4\%$ (▲) and $\varepsilon = 0.62\%$ (◇). Inset shows the same curves without normalization.

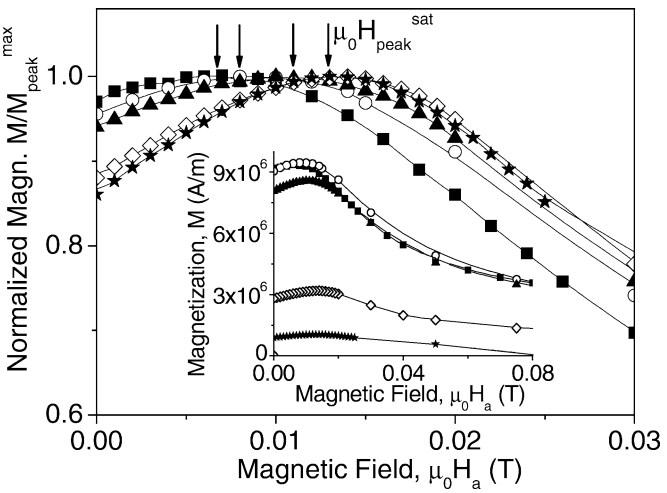

Fig. 3. Saturated reverse branches of the magnetization curves normalized to the corresponding magnetization value at the peak position, obtained for the IBAD-CC at 77 K, as grown (■) and after consecutive bendings with induced deformations of $\varepsilon = 0.63\%$ (∘), 0.8% (▲), 1.25% (◇) and 2.6% (⋆). Inset shows the same curves without normalization.

and 2.6%, respectively. Moreover the saturation of the grain magnetization takes place at lower magnetic fields after each deformation, $\mu_0 \mathrm{H_m}^{\mathrm{sat}} \sim 0.04$ T, 0.035 T and 0.028 T for $\varepsilon = 0\%$, 0.8% and 2.6%, respectively. The different values obtained for $\mu_0 \mathrm{H_{peak}}^{\mathrm{sat}}$ and $\mu_0 \mathrm{H_m}^{\mathrm{sat}}$ result in variations of $\mathrm{J_c}^{\mathrm{G}}$ and grain size, during the deformation process performed to the IBAD tape, contrary to that observed in the RABiTS-CC. Fig. 4 shows the average grain size obtained for RABiTS and IBAD CCs as a function of the applied bending strain. As we have mentioned above, the average grain size stays constant when the bending process is applied to the RABiTS-CC, $\langle 2a \rangle \sim 25\ \mu\mathrm{m}$, and no change is observed in $\mathrm{J_c}^{\mathrm{G}} = 3.4\ \mathrm{MA/cm^2}$ (Fig. 5). A totally different situation is found in the IBAD conductor, since the calculated average grain size increases with the deformation tests and at the same time $\mathrm{J_c}^{\mathrm{G}}$ decreases. The behavior observed with the IBAD-CC can be understood if one assumes

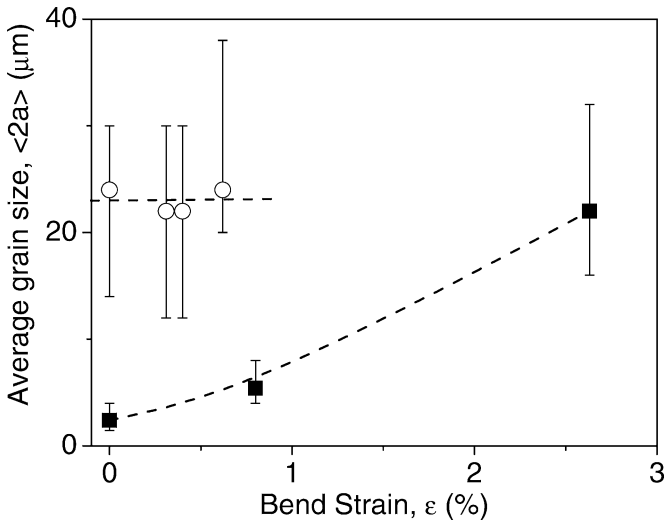

Fig. 4. Average grain size, $\langle 2a \rangle$, determined for the RABiTS-CC (∘) and IBAD-CC (■) as a function of bend strain.

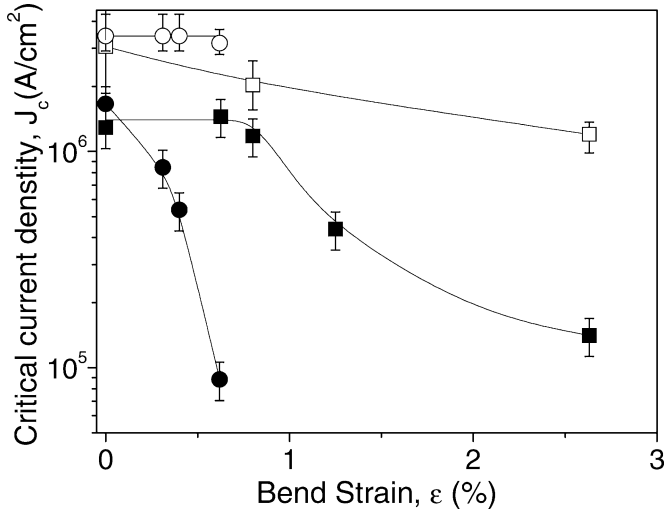

Fig. 5. $\mathrm{J_c}^{\mathrm{G}}$ (open symbols) and $\mathrm{J_c}^{\mathrm{GB}}$ (closed symbols) for the RABiTS-CC (•) and IBAD-CC (■) as a function of the bend strain.

that after bending, the grain boundary network becomes inhomogeneous, producing grain boundaries of different quality. The strain deformation could deteriorate some of the high angle grain boundaries (HAGB) between the structural grains generating clusters (colonies) of well connected grains surrounded with current loops with a somewhat degraded critical current density, $\mathrm{J_c}^{\mathrm{col}}/\mathrm{J_c}^{\mathrm{G}} \sim 0.7$ for $\varepsilon = 0.8\%$. Therefore the final percolative current crossing the sample, would be affected by the return field of structural grains and grain colonies. By performing simulations based on the critical state model [11] we have obtained that 35% of isolated colonies of 10 μm in a matrix of small grains (2 μm) are able produce the effect observed on the hysteresis loops for $\varepsilon = 0.8\%$. Comparing the values of $\mathrm{J_c}^{\mathrm{GB}}$ obtained for both type of CCs after deformation tests (Fig. 5), one observes that the most rapid degradation of $\mathrm{J_c}^{\mathrm{GB}}$ occurs for the RABiTS-CC, for instance, $\mathrm{J_c}^{\mathrm{GB}}$ is reduced by 50% when we apply a deformation of $\varepsilon = 0.32\%$ in the RABiTS-CC while for the IBAD-CC we have to apply a deformation of $\varepsilon = 1\%$. These results indicate that the strain

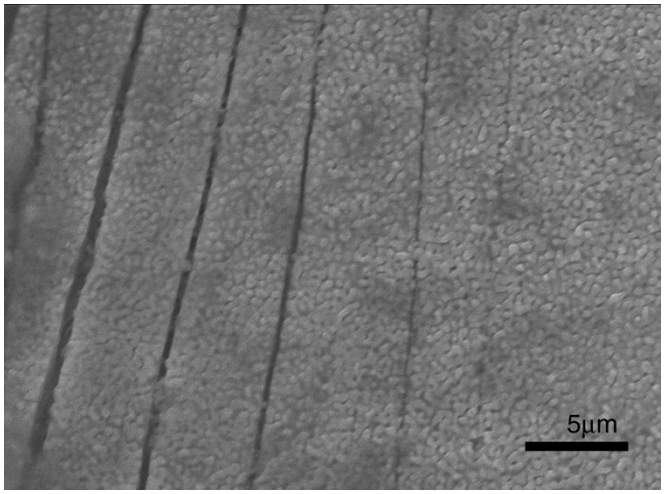

Fig. 6. SEM image of the RABiTS film after three consecutive bendings with induced deformations of $\varepsilon = 0.32\%$, 0.4% and 0.62%. Transverse cracks can be observed in some regions of the sample, caused by tensile.

tolerance of the YBCO layer grown on a Ni-Cr stainless steel IBAD substrate is greater than that of the YBCO layer grown on a 3%W-RABiTS tape. The degradation of $J_c{}^{GB}$ is known to increase with increasing the total multilayer thickness [5]. As we have analyzed a thicker IBAD CC than RABiTS CC and we have still obtained better mechanical properties in the IBAD CC, we can strongly conclude that IBAD CC possesses a better strain tolerance than RABiTS CC. The reduction in $J_c{}^{GB}$, observed in both samples, clearly evidences that the grain boundary network of the YBCO layer has been damaged when the tape is submitted to strain deformation. Fig. 6 shows a scanning electron microscopy (SEM) image of the RABiTS tape, after all the sequence of bending tests corresponding to a $J_c{}^{GB}(\varepsilon = 0.62\%)/J_c{}^{GB}(\varepsilon = 0\%) \sim 0.05$, where one can clearly identify the formation and propagation of transverse cracks in some regions of the sample, which confirms the degradation of the percolative critical current and evidences the importance of controlling the mechanical properties of these materials.

IV. Conclusion

The effects of strain bending deformation on $J_c{}^{G}$ and $J_c{}^{GB}$ have been studied in YBCO coated conductors. We have identified a clear degradation of $J_c{}^{GB}$ after bending test wile $J_c{}^{G}$ stays constant. Moreover, for the IBAD-CC analyzed inhomogeneities on the GB network can be detected after bending. A different strain tolerance has been observed for RABiTS and IBAD CCs. For the IBAD sample $J_c{}^{GB}$ maintains a 90% of its original value when $\varepsilon < 1\%$, while for the RABiTS sample $\varepsilon = 0.32\%$ already reduces $J_c{}^{GB}$ by 50%. On the other hand, recent axial strain measurements have shown a reversible strain limit for RABiTS of $\sim$0.4% [7]. The present results indicate that reinforcement may be required for RABiTS samples in applications involving extreme bending configurations.

Acknowledgment

A. Palau wishes to acknowledge MCyT for a doctoral fellowship.

References

[1] D. M. Feldmann, J. L. Reeves, A. A. Polyanskii, G. Kozlowski, R. R. Biggers, R. M. Nekkanti, I. Maartense, M. Tomsic, P. Barnes, C. E. Oberly, T. L. Peterson, S. E. Babcock, and D. C. Larbalestier, "Influence of nickel substrate grain structure on $YBa_2Cu_3O_{7-x}$ supercurrent connectivity in deformation-textured coated conductors," *Appl. Phys. Lett.*, vol. 77, pp. 2906–2908, 2000.

[2] D. M. Feldmann, D. C. Larbalestier, D. T. Verebelyi, W. Zhang, Q. Li, G. N. Riley, R. Feenstra, A. Goyal, D. F. Lee, M. Paranthaman, D. M. Kroeger, and D. K. Christen, "Inter- and intragrain transport measurements in $YBa_2Cu_3O_{7-x}$ deformation textured coated conductors," *Appl. Phys. Lett.*, vol. 79, pp. 3998–4000, 2001.

[3] D. T. Verebelyi, D. K. Christen, R. Feenstra, C. Cantoni, A. Goyal, D. F. Lee, M. Paranthaman, P. N. Arendt, R. F. DePaula, J. R. Groves, and C. Prouteau, "Low angle grain boundary transport in $YBa_2Cu_3O_{7-\delta}$ coated conductors," *Appl. Phys. Lett.*, vol. 76, pp. 1755–1757, 2000.

[4] H. C. Freyhardt, J. Hoffmann, J. Wiesmann, J. Dzick, K. Heinemann, A. Issaev, A. Usoskin, and F. Garcia-Moreno, "Y-123 films on technical substrates," *Appl. Supercond.*, vol. 4, pp. 435–446, 1996.

[5] C. Park, D. P. Norton, J. D. Budai, D. K. Christen, D. Verebelyi, R. Feenstra, D. F. Lee, A. Goyal, D. M. Kroeger, and M. Paranthaman, "Bend strain tolerance of critical currents for $YBa_2Cu_3O_7$ films deposited on rolled-textured, (001)Ni," *Appl. Phys. Lett.*, vol. 73, pp. 1904–1906, 1998.

[6] D. C. van der Laan, H. J. N. van Eck, B. ten Haken, H. H. J. ten Kate, and J. Schwartz, "Strain effects in high temperature superconductors investigated with magneto-optical imaging," *IEEE Trans. Appl. Supercond.*, vol. 13, pp. 3534–3539, 2003.

[7] N. Cheggour, J. W. Ekin, C. C. Clickner, D. T. Verebelyi, C. L. H. Thieme, R. Feenstra, and A. Goyal, "Reversible axial-strain effect and extended strain limits in Y-Ba-Cu-O coatings on deformation-textured substrates," *Appl. Phys. Lett.*, vol. 83, pp. 4223–4225, 2003.

[8] R. Feenstra *et al.*, , 2004, unpublished.

[9] A. Usoskin, J. Knoke, F. Garcia-Moreno, A. Issaev, J. Dzick, S. Sievers, and H. C. Freyhardt, "Large-area HTS-coated stainless steel tapes with high critical currents," *IEEE Trans. Appl. Supercond.*, vol. 11, pp. 3385–3388, 2001.

[10] A. Palau, T. Puig, X. Obradors, A. Usoskin, H. C. Freyhardt, L. Fernandez, and B. Holzapfel, "Inductive analysis of magnetic granularity effects in YBCO IBAD and RABiTS coated conductors," *IEEE Trans. Appl. Supercond.*, vol. 13, pp. 2599–2602, 2003.

[11] A. Palau *et al.*, , 2004. Unpublished.

[12] B. Holzapfel, L. Fernandez, F. Schindler, B. De Boer, N. Reger, J. Eickemeyer, P. Berberich, and W. Prusseit, "Grain boundary networks in Y-123 coated conductors: formation, properties and simulation," *IEEE Trans. Appl. Supercond.*, vol. 11, pp. 3872–3875, 2001.

[13] C. Jooss, L. O. Kautschor, M. P. Delamare, B. Bringmann, K. Guth, V. Born, S. Sievers, H. Walter, J. Dzick, J. Hoffmann, H. C. Freyhardt, B. De Boer, B. Holzapfel, and F. Sandiumenge, "Magneto-optical study of grain boundaries, interfaces and grain boundary networks in YBaCuO," in *Mat. Res. Soc. Symp. Proc.*, vol. 659, 2001.